

# Video-based Locomotion Analysis for Fish Health Monitoring

Timon Palm<sup>1</sup><sup>a</sup>, Clemens Seibold<sup>1,2</sup><sup>b</sup>, Anna Hilsmann<sup>1</sup><sup>c</sup> and Peter Eisert<sup>1,2</sup><sup>d</sup>

<sup>1</sup>Fraunhofer HHI, Berlin, Germany

<sup>2</sup>Humboldt University of Berlin, Berlin, Germany

{timon.palm, clemens.seibold, anna.hilsmann, peter.eisert}@hhi.fraunhofer.de

Keywords: Multi Object Tracking, Tracking-By-Detection, Fish Tracking, Fish behavior monitoring

Abstract: Monitoring the health conditions of fish is essential, as it enables the early detection of disease, safeguards animal welfare, and contributes to sustainable aquaculture practices. Physiological and pathological conditions of cultivated fish can be inferred by analyzing locomotion activities. In this paper, we present a system that estimates the locomotion activities from videos using multi object tracking. The core of our approach is a YOLOv11 detector embedded in a tracking-by-detection framework. We investigate various configurations of the YOLOv11-architecture as well as extensions that incorporate multiple frames to improve detection accuracy. Our system is evaluated on a manually annotated dataset of *Sulawesi ricefish* recorded in a home-aquarium-like setup, demonstrating its ability to reliably measure swimming direction and speed for fish health monitoring. The dataset will be made publicly available upon publication.

## 1 INTRODUCTION

Image-based fish tracking algorithms play a central role in digital aquaculture, enabling the monitoring of various aspects related to the welfare and reproductive behavior of cultured fish. Accurate tracking of individual fish and entire shoals facilitates detailed behavioral analysis, which is essential for effective aquaculture management.

Quantitative locomotion features derived from trajectories can provide important indicators of fish health. Average speed, burst patterns, acceleration, body orientation, and swimming direction can reveal subclinical stress or pathology. For example, electrical leakage currents, which can arise from malfunctioning equipment, can cause neuromuscular injuries, resulting in loss of equilibrium. This can manifest as abnormal swimming behavior with erratic bursts and atypical locomotion in vertical directions (Moccia, 1991). Swimming performance is widely used as a health and welfare parameter in aquaculture (Leatherland and Woo, 2006) and helps to detect diseases and disorders at an early, treatable stage. The often-occurring swim bladder disease, for example, can be caused by various factors such as infection, overfeed-

ing, incorrect water temperature, and stress manifests. It usually results in abnormal swimming, causing fish to float up and down instead of swimming horizontally (Roberts, 2023).

Vision-based (i.e., image- and video-based) tracking approaches are particularly attractive due to their simple setup, low cost, durability and no interference with the fish, compared to alternative sensing modalities (e.g., acoustic or biosensor-based systems).



Figure 1: The *Sulawesi ricefish*: Its lucid appearance, small size and the large number of instances in a shoal makes accurate tracking difficult.

Multi-Object Tracking (MOT) has been an active research field in computer vision (Luo et al., 2021) and has been applied to various tracking problems (e.g. cars (Koller et al., 1994) or pedestrians (Yang et al., 2011)). However, tracking fish in their natural environment poses significant challenges for vision-based systems, as fish are frequently occluded, interact with one another, change direction rapidly, and un-

<sup>a</sup> <https://orcid.org/0009-0003-6016-7718>

<sup>b</sup> <https://orcid.org/0000-0002-9318-5934>

<sup>c</sup> <https://orcid.org/0000-0002-2086-0951>

<sup>d</sup> <https://orcid.org/0000-0001-8378-4805>

dergo continuous morphological deformation due to their non-rigid bodies. Furthermore, unlike humans, fish often exhibit high visual similarity, making individual discrimination more difficult.

However, extracting such behavioral indicators requires consistent long-term detection and tracking of individual fish in complex environments.

In this work, we build upon the classical Tracking-By-Detection (TbD) paradigm and enhance YOLO-based detectors by increasing the input channels to allow multi-frame input training. Inspired by recent results showing that multi-frame conditioning can substantially improve detection of small or partially occluded pedestrians (Quan et al., 2025), we investigate whether similar design principles benefit fish tracking in dense aquaculture scenes. Our evaluation focuses on the challenging *Sulawesi ricefish* whose small size and large shoal densities make them a representative benchmark in controlled culture conditions (see Figure 1).

Based on the tracking, we derive the distribution of swimming directions for fish shoal in videos, which facilitates the assessment of excessive up and down swimming behavior. This is schematically visualized in Figure 2.

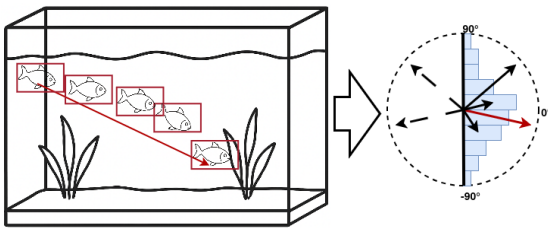


Figure 2: A schematic view of extracting quantitative directional information of fish observations from Tracking-By-Detection methods.

Our contributions are threefold

- A curated hand-labeled video dataset of *Sulawesi ricefish* shoals recorded under controlled aquaculture conditions, providing a fish tracking benchmark with complex scenarios, such as rapid direction changes, frequent occlusions, etc. (Dataset: <https://cvg.hhi.fraunhofer.de/>)
- A qualitative evaluation of multi-frame YOLO adaptations for detecting and tracking fish shoals, examining the impact of incorporating different relative context frames in combination with various YOLO model scales.
- A pipeline for the derivation of quantitative locomotion features from fish trajectories as a health indicator.

## 2 RELATED WORK

A common class of trackers uses the framework of TbD, which splits the task in two stages: first, detecting bounding boxes with Deep Learning models and then using an autoregressive filter (e.g., Kalman filter (Kalman, 1960)) to propagate instances of detected bounding boxes over time. Other types of Deep Learning trackers, such as Joint Detection and Embedding (JDE), jointly learn the detection and tracking phases by extracting object specific embeddings. JDEs show strong performance for tracking crowds or vehicles, but generally fail to track fish due to their frequent occlusion and inconsistent scales and shapes (Li et al., 2022).

Bytetrack (Zhang et al., 2021) and BoT-SORT (Aharon et al., 2022) are two simple yet widely used TbD methods. Both methods use the Kalman filter (Kalman, 1960) as their core motion model. While previous methods (Wang et al., 2018; Du et al., 2022a) incorporated additional appearance feature in the data association, Bytetrack and BoT-SORT rely solely on high-performing detection models and their detection scores. High confidence detections are prioritized in the matching process, while low scoring detections are not entirely discarded but instead considered in a secondary association stage.

The success of detection-only trackers is crucially dependent on the performance of the detection model. The YOLO architecture (Redmon et al., 2016) provides a powerful yet lightweight detection model for real-time trackers. It shows superior performance compared to other models such as Faster R-CNN (Liu et al., 2024). Further advancements include YOLO tracking endowed with a CNN for modeling the appearance features of fish (Wojke et al., 2017), its successor incorporates a ResNet-50 backbone (Du et al., 2022b).

(Quan et al., 2025) showed that by minimally modifying the YOLOv7 detection model to accommodate multi-frame inputs, the accuracy and robustness of the detections could be improved up to 8 percentage points (pp), in particular for lightweight-model versions. Formally, given a sequence of  $T$  RGB video frames  $\{I_t\}_t^T$  with  $I_t \in \mathbb{R}^{N \times M \times 3}$ , instead of predicting detections for frame  $I_t$  only on its information, you concatenate  $n$  consecutive frames channel-wise and thereby provide the model with a short time-window of frames  $\{I_{t-n+1}, \dots, I_t\}$ , resulting in the input shape  $(N, M, 3 \times n)$ . Standard convolution is jointly applied across all channels, enabling the integration of spatial-temporal features from the very first layer.

Larger steps in between frames broaden the tem-

poral context available for the model without engorging the channels. This has been shown to be crucial for maximizing the robustness using three to seven frames  $n \in \{3, 7\}$  as context window size (Quan et al., 2025).

However, the multi-frame YOLO model used for tracking has thus far only been evaluated on pedestrian-tracking tasks. Its capability to handle complex multi-fish tracking scenarios involving frequent occlusions and pronounced morphological variations remains unknown.

The exhaustive study on imaging technologies for fish behavior analysis by (Cui et al., 2025) has revealed that Bytetrack and BoT-SORT are particularly suitable for the application of fish tracking in different scenarios. However, they further emphasize that comprehensive and unified tracking performance assessment is limited due to a paucity of appropriate datasets. The available datasets either have very low resolution or consist of videos recorded in simplified environments, such as observation tanks with shallow water, uniform backgrounds, and no aquatic plants.

### 3 METHOD

The extraction of quantitative directional properties of a fish shoals motion with TbD trackers takes three stages: mere detection of instances from imagery, tracking the detection across frames and the computation of directional motion. A schematic illustration of the procedure is shown in Figure 2.

Accurate fish detection from single imagery has its limitations, where fish occlude each other, are blurry due to rapid motion or are poorly illuminated. Intuitively, detection models should benefit from extended temporal context, which enables them to exploit inter-frame differences and fish-specific motion patterns as cues that distinguish fish from other objects.

YOLOv11 (Khanam and Hussain, 2024) is a fast and flexible object detection model that predicts object classes and locations in a single pass through the full image, representing a significant advancement in real-time detection performance. The model comprises a Convolutional Neural Network (CNN)-based feature extraction backbone and multiple task-specific heads for detection and classification. Extending the channel dimension of the first convolutional layer to accommodate multi-frame input represents a minimal architectural modification that introduces only a negligible increase in parameters. Nevertheless, this adjustment allows the model to exploit temporal information already in the early stages of feature extrac-

tion.

In the following, we denote the focus frame, for which the fish detection is performed, as  $\mathbf{X}$ . Additional frames included in the temporal context are denoted as  $\mathbf{x}$ , whereas  $\_$  indicates frames that are omitted. For example, the context scheme  $\mathbf{x}\_ \mathbf{X} \mathbf{x}$  represents a window size of three frames, where one preceding and one subsequent frame are included, while the frames immediately adjacent to the focus frame are skipped.

The detection models are applied within the Bytetrack and BoT-SORT framework without further modifications, to obtain consistent identity tracks. TbD trackers have shown to be powerful, yet lightweight enough for precise tracking in moderate conditions, provided with a sufficiently accurate detection model.

Building on fish trajectories, we further analyze the motion characteristics of the detected individuals by estimating their swimming directions.

We create a direction estimate for each individual fish by gathering the displacements per frame. Thereby, we obtain  $n - 1$  directions, including the swimming magnitude. Furthermore, we mirror all directions on the vertical axis to one side to eliminate the horizontal directions and to ultimately obtain the angular direction in a degree range of  $-90^\circ$  (orthogonal downwards) and  $90^\circ$  (orthogonal upwards).

For noise-reduction purpose, we discarded all trajectories shorter than 5 frames and took the mean direction over 5 frames.

For each video, we obtain a distribution of swimming angles across all fish, which can reveal abnormalities in the collective swimming behavior of the shoal. Under normal conditions, the average swimming direction is predominantly horizontal, and the angle distribution should therefore peak at  $0^\circ$  and gradually taper toward both sides. Pronounced peaks away from the center indicate substantial upward or downward motion.

### 4 DATASET

To facilitate automated analysis of Sulawesi ricefish behavior, we curated a novel dataset for tracking and segmentation. We recorded videos of a fish tank at an institution focused on preserving maritime biodiversity through cultivation of endangered fish species. The videos were captured with a Basler a2A2448-75ucPRO and a 6mm lens from multiple viewpoints around the tank, with the camera perpendicular targeting glass wall. The videos have a resolution of 2448 x 2048 pixels at 30 frames per second. The environment resembles a typical home aquarium, with



Figure 3: Example frames with segmentation annotation from our *Sulawesi ricefish* dataset.

the main light source above the tank.

The dataset contains two annotated video sequences for evaluation (202 frames in total). For training, we have annotated 37 additional frames, picked at random from different video sequences to provide frames with fish positions independent of each other. Figure 3 shows two example frames with annotations from the dataset.

Each frame was semi-automatically annotated to generate pixel-level segmentation masks of individual fish and identity-preserving tracking labels across frames, thereby making the dataset suitable for both segmentation and tracking tasks. It captures a wide range of postures, swimming speeds, and inter-individual occlusions, providing a valuable benchmark for multi-object tracking and instance segmentation algorithms in aquatic environments (see Table 1 for a summary).

Table 1: A summary of the *Sulawesi ricefish* dataset specification for video A and B

Video	Fish Count	#Tracks	Fish per Frame (avg)
<b>A</b>	9214	256	~ 91.2
<b>B</b>	1969	45	~ 19.5

We encourage its use in developing and evaluating computer vision models for fish behavior analysis.

## 5 EXPERIMENTS

We conducted a series of experiments on our *Sulawesi ricefish* dataset to evaluate the tracking accuracy of ByteTrack and BoT-SORT, using context-modified detection models of varying sizes. From the resulting trajectories, swimming direction and speed are derived as potential indicators of the fishes’ health condition. Since both ByteTrack and BoT-SORT operate on bounding boxes, we use the smallest enclosing rectangles of the annotated segmentation masks

provided in the dataset.

In Section 5.1, we examine the impact of using multiple input frames on the detection results by fine-tuning the YOLOv11 model (Khanam and Hussain, 2024). The best-performing detection models are subsequently employed in Section 5.2 within ByteTrack and BoT-SORT to evaluate the tracking accuracy and to assess their suitability for estimating the speed and directional dynamics of fish swimming behavior in Section 5.3.

### 5.1 Detection

To evaluate the effect of increasing the temporal context of the YOLOv11 detection, we have considered context window sizes of three and five frames, as well as the effect of omitting frames that are directly adjacent to the center frame. We primarily focus on symmetric temporal windows, as these help constrain the space of plausible bounding box predictions, thereby supporting more stable model learning. We also include an asymmetric window configuration as a reference. An overview of the context window configurations used in this study can be taken from Table 2.

The weights of the convolutional filters of the additional channels’ are randomly initialized with values  $w \sim \mathcal{N}(0, 0.01)$ . The model should still primarily use the information provided by the frame to get the detections for, and only take advantage of features improving its detections from surrounding frames. We evaluated the modification on the YOLOv11 nano (2.6 M parameters), medium (9.4 M parameters), and large (20.1 M parameters) variant, all of which employ a  $3 \times 3$  convolutional kernel in the first layer.

The training set of the fish recordings was split into 33 training frames and 4 validation frames. We used the recommended default training parameters and setting from (Jocher and Qiu, 2024) with a modified box loss factor of  $box = 10$  to emphasize the training on accurate detections rather than the class accuracy, as we only have one in this case.

Table 2: Precision, Recall, mAP50 (Everingham et al., 2015) and mAP50-95 (Lin et al., 2014) metrics for each context configuration in our experiments. Best values are shown in bold, second best are underlined.

Scheme	Model Size	Precision $\uparrow$	Recall $\uparrow$	mAP50 $\uparrow$	mAP50-95 $\uparrow$
<b>SingleFrame</b>	nano	0.840	0.850	0.885	0.580
	medium	0.850	0.860	0.890	0.590
	large	0.851	0.849	0.892	0.595
<b>xxX</b>	nano	0.858	0.750	0.830	0.530
	medium	0.884	0.773	0.844	0.563
	large	0.913	0.733	0.845	0.557
<b>xXx</b>	nano	0.895	0.815	0.887	0.548
	medium	0.941	0.802	0.912	0.588
	large	0.855	0.782	0.869	0.547
<b>xxXxx</b>	nano	0.892	0.844	0.911	0.608
	medium	0.899	0.857	0.928	0.628
	large	0.828	0.872	0.910	0.614
<b>x_X_x</b>	nano	0.881	0.820	0.882	0.601
	medium	0.882	0.878	0.920	0.645
	large	0.933	0.805	0.896	0.588
<b>x_X_x_pt</b>	pre-trained	<b>0.983</b>	<b>0.879</b>	<b>0.963</b>	<b>0.766</b>

Training was conducted for 300 epochs on a single *NVIDIA RTX 6000* GPU and required approximately 10 minutes for the largest model.

### 5.1.1 Metrics

Assessing the performance of object detections to ground-truth data requires the assignment of each proposal bounding box to a true detection. This optimal bipartite assignment problem is solved by the Hungarian algorithm with Intersection-Over-Union (IoU) values as weights and a threshold of  $iou > 0.5$ . Unassigned ground-truth bounding boxes count as False-Negative (FN), whereas unassigned proposals count as False-Positives (FP).

Precision measures the proportion of correctly detected bounding boxes among all predicted boxes, whereas recall quantifies the proportion of true fish instances successfully detected in the scene. While these provide fundamental quantitative indicators, we further assess detection accuracy using the mAP50 and mAP50-95 metrics, which integrate precision and recall as average precision under IoU thresholds of 0.5 and from 0.5 to 0.95, respectively. The mAP50-95 metric serves as a stricter measure, reflecting both the localization and size accuracy of the predicted bounding boxes.

### 5.1.2 Results

Table 2 summarizes the detection results. Overall, larger temporal windows tend to yield better performance (best and second-best results are shown in bold and underlined, respectively). Interestingly, the model *x\_X\_x* with omitted frames performs on par

to the full context window model *xxXxx*, suggesting that temporal sparsity does not necessarily harm detection accuracy. While individual configurations show notable gains, e.g. *x\_X\_x* model m (up to 5.5 pp better than single frame in mAP50-95), no universally consistent trend emerges across all architectures. The temporal context *x\_X\_x* for example, shows great improvement in composition with the YOLO model in size medium, whereas it provides little to no improvement for the large model. Generally, the model size medium performed best throughout all context schemes.

The reference with asymmetric context (*xxX*) performed worse in all experiments, even worse than the single-frame baseline. This confirms the assumption that symmetric context windows are beneficial, whereas context windows that extend only into the past are, in fact, detrimental.

Additionally, to further examine the potential improvement in detection accuracy, we initialized the best-performing context-type model (*x\_X\_x*) using the weights of our reference single-frame model rather than the default YOLOv11 weights. This variant is denoted as *x\_X\_x\_pt* in Table 2. Taking the pre-trained weights on our fish dataset had an impressive effect on the detection precision, yielding gains of 5 pp over the *x\_X\_x* configuration and 13 pp over the single frame baseline, and resulting in the highest mAP50-95 score of 76.6% in our experiments. Interestingly, although detection accuracy increased, recall only improved marginally (1-2 pp improvement over baseline). It is important to note, however, that pre-training the single frame model and later using those weights to increase the context size, subjects

the model to two optimization phases on the same dataset. As a result, this configuration undergoes roughly twice as many optimization steps as the other models in the comparison.

For evaluating the tracking with ByteTrack and BoT-SORT, we only considered the models  $x\_X\_x$ ,  $x\_X\_x\_pt$ ,  $xXx$ , as well as the single frame reference model. Again, we conducted experiments on all three YOLOv11 sizes.

## 5.2 Tracking

Improving the accuracy of bounding box detection models for TbD tracker does not necessarily improve the tracking itself. With this experiment, we examine how much TbD trackers can benefit from our improved detection models for fish tracking. We have used the two very commonly applied TbD methods ByteTrack (Zhang et al., 2021) and BoT-SORT (Aharon et al., 2022) on our *Sulawesi ricefish* dataset, containing two videos. We used the detection models  $x\_X\_x$ ,  $x\_X\_x\_pt$ ,  $xXx$  and the single frame reference model. Additionally, we ran both tracking methods on the ground-truth detections to set an upper limit for the tracking performance. The default parameters from Ultralytics (Jocher and Qiu, 2024) are taken for ByteTrack and BoT-SORT.

### 5.2.1 Metrics

Based on the detection assignments described in Section 5.1.1, we evaluate the quality and consistency of the tracking results using three MOT metrics, which have been commonly applied in previous work (Zhang et al., 2021; Aharon et al., 2022). Each metric captures a distinct aspect of tracking performance:

- **IDF1** (Ristani et al., 2016) is defined as the harmonic mean of the identity precision and identity recall. It quantifies the consistency of object identities across frames. Unlike traditional frame-based precision and recall, IDF1 considers temporal consistency, penalizing identity switches and fragmented tracks. High IDF1 values indicate that the tracker maintains stable and consistent identities across frames.
- **MOTA** (Multiple Object Tracking Accuracy) is part of the CLEAR metrics (Bernardin and Stiefelhagen, 2008) measuring the overall tracking accuracy by jointly accounting for missed detections (FN), False-Positives and identity switches. Although MOTA offers a single scalar summarizing overall performance, it is known to be dominated by detection quality and may underrepresent the impact of identity fragmentation

(Luiten et al., 2020). Nonetheless, it remains a standard benchmark for evaluating multi-object trackers due to its interpretability and comparability.

- **HOTA** (Higher Order Tracking Accuracy) (Luiten et al., 2020) provides a balanced and comprehensive measure of accurate detection, association and localization. It is defined as the geometric mean of detection accuracy (detection accuracy (DetA)) and association accuracy (association accuracy (AssA)), thereby integrating both the per-frame and temporal aspects of tracking.

To further contextualize these tracking metrics, we relate them to mAP50–95, a detection-only performance measure that reflects the average precision across multiple IoU thresholds.

### 5.2.2 Results

Tables 3 and 4 summarize the tracking results obtained using ByteTrack and BoT-SORT, respectively. For video B, the model with the  $x\_X\_x$  context window in size medium consistently outperforms all other models across each metrics, regardless of the tracking algorithm. In contrast, the results for video A are less pronounced. While the same model still performs well relative to others, it does not achieve the highest scores on every metric. Interestingly, the nano model variant achieved slightly higher IDF1 and HOTA scores for video A with ByteTrack, though the improvement was modest (1–3 pp).

With the exception of  $x\_X\_x\_pt$ , the large model variant consistently performed worse. This is likely attributable to overfitting to the training data, as its detection mAP50-95 on both test videos is markedly lower than that of all other models, including the single-frame reference, despite achieving the highest validation performance during training.

Providing larger context windows  $x\_X\_x$  could improve the general detection accuracy (mAP50-95) in the dataset up to 9 pp and therefore, leads to better tracking results, too. Though, the tracking improvements measure by IDF1, MOTA and HOTA are only about 1 pp.

Nevertheless, the tracking results are not consistent among model sizes. Although in general the medium model performed better than small, the large model performed worse, in some instances even worse than the nano single frame reference.

A clear performance gap persists relative to tracking with ground-truth detections, mainly driven by inaccurate or missing detections. Under ground-truth detection conditions, ByteTrack and BoT-SORT

Table 3: Bytetrack: Tracking results for using different context windows for the YOLOv11 detection model. The best performance is highlighted in bold and the second best is underlined.

Scheme	Size	Video A				Video B			
		mAP50-95 $\uparrow$	IDF1 $\uparrow$	MOTA $\uparrow$	HOTA $\uparrow$	mAP50-95 $\uparrow$	IDF1 $\uparrow$	MOTA $\uparrow$	HOTA $\uparrow$
<b>GT Detections</b>	-	1.000	0.756	0.991	0.803	1.000	0.815	0.981	0.856
<b>Single Frame</b>	nano	0.451	0.396	0.165	0.330	0.368	0.486	0.360	0.373
	medium	0.413	0.465	0.005	0.374	0.442	0.461	0.265	0.362
	large	0.416	0.439	0.012	0.361	0.370	0.427	0.193	0.339
<b>xXx</b>	nano	0.445	0.539	0.331	0.408	0.398	0.463	0.363	0.346
	medium	<b>0.502</b>	0.559	0.368	<u>0.428</u>	0.420	0.451	0.339	0.341
	large	0.413	0.442	0.130	<u>0.362</u>	0.281	0.390	0.196	0.301
<b>x_X_x</b>	nano	0.447	<b>0.583</b>	0.357	<b>0.433</b>	0.406	0.432	0.327	0.334
	medium	0.493	0.554	<b>0.384</b>	0.419	<b>0.477</b>	<b>0.492</b>	<b>0.409</b>	<b>0.375</b>
	large	<u>0.420</u>	0.485	0.112	0.390	0.374	0.426	0.284	0.329
<b>x_X_x_pt</b>	nano	0.404	0.405	0.106	0.336	0.431	0.482	0.382	0.374
	medium	0.363	0.456	0.368	0.367	0.300	0.358	0.147	0.288
	large	0.471	<u>0.560</u>	<u>0.370</u>	0.422	<u>0.455</u>	0.472	<u>0.387</u>	0.361

Table 4: BoT-SORT: Tracking results for using different context windows for the YOLOv11 detection model. The best performance is highlighted in bold and the second best is underlined.

Scheme	Size	Video A				Video B			
		mAP50-95 $\uparrow$	IDF1 $\uparrow$	MOTA $\uparrow$	HOTA $\uparrow$	mAP50-95 $\uparrow$	IDF1 $\uparrow$	MOTA $\uparrow$	HOTA $\uparrow$
<b>GT Detections</b>	-	1.000	0.756	0.991	0.803	1.000	0.824	0.976	0.856
<b>Single Frame</b>	nano	0.451	0.407	0.071	0.361	0.368	0.532	0.455	0.423
	medium	0.413	0.507	0.130	0.428	0.442	0.509	0.383	0.421
	large	0.416	0.489	0.099	0.422	0.370	0.489	0.313	0.400
<b>xXx</b>	nano	0.445	0.604	0.363	0.481	0.398	0.493	0.427	0.386
	medium	<b>0.502</b>	0.616	0.485	<b>0.494</b>	0.420	0.507	0.407	0.396
	large	0.413	0.517	<u>0.250</u>	0.432	0.281	0.440	0.266	0.340
<b>x_X_x</b>	nano	0.447	<b>0.625</b>	0.479	0.483	0.406	0.482	0.392	0.390
	medium	<u>0.493</u>	0.606	<b>0.507</b>	0.474	<b>0.477</b>	<b>0.534</b>	<b>0.503</b>	<b>0.429</b>
	large	0.420	0.538	0.253	0.435	0.374	0.460	0.345	0.378
<b>x_X_x_pt</b>	nano	0.404	0.470	0.031	0.397	0.431	0.520	0.463	0.420
	medium	0.363	0.486	0.072	0.410	0.300	0.395	0.212	0.320
	large	0.471	<u>0.623</u>	0.474	<u>0.491</u>	<u>0.455</u>	0.516	<u>0.464</u>	0.408

reach HOTA scores of up to 85 %.

### 5.3 Swimming Direction

In this section, we evaluate the reliability and credibility of the swimming direction estimates produced by TbD trackers, with a focus on their suitability for fish health monitoring.

Due to noise-reduction by discarding very short trajectories, the number of resulting direction vectors is lower than in the ground-truth. Nevertheless, if the tracking is accurate, the overall directional distribution should remain similar to the ground-truth, even though each direction effectively contributes a higher weight.

The results of this analysis are depicted in Figure 4, showing the swimming direction distribution for video A and B from our *Sulawesi ricefish* dataset. We examined the directions of all context variants

from the tracking in Section 5.2 and all three model sizes (nano, medium and large).

Figure 5 shows the distribution of the swimming magnitude (speed) in pixel space over 5 frames. The results are similar to the direction analysis. All model variations are close to the ground-truth, however all variants have larger portion of low magnitude estimates, in particular for video B.

Overall, we can say that the derived directional estimates of the fish motion are sufficiently close to the true directional estimate for all studied model variants, with only a few exceptions (x\_X\_x\_pt in size medium in video A). This is a surprising result: that improving the fish tracking by using larger context windows, the assessment of the swimming directions and magnitude is little affected. Even the classic single frame tracking suffices as a method for computing the directions in a holistic view.

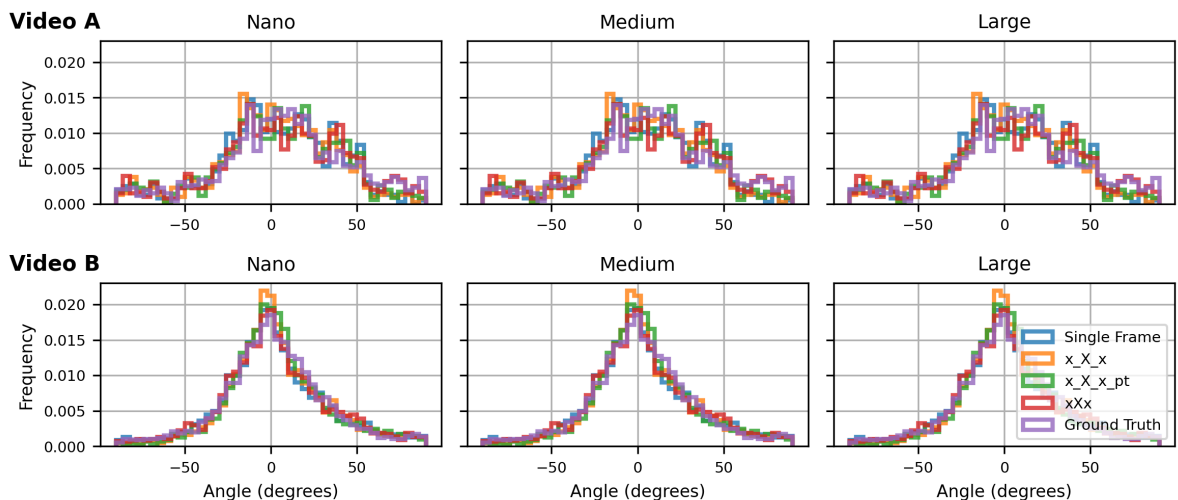


Figure 4: Histograms depicting the angular swimming directions extracted from tracking with model size nano (left), medium (middle) and large (right) for video A (top row) and video B (bottom row).

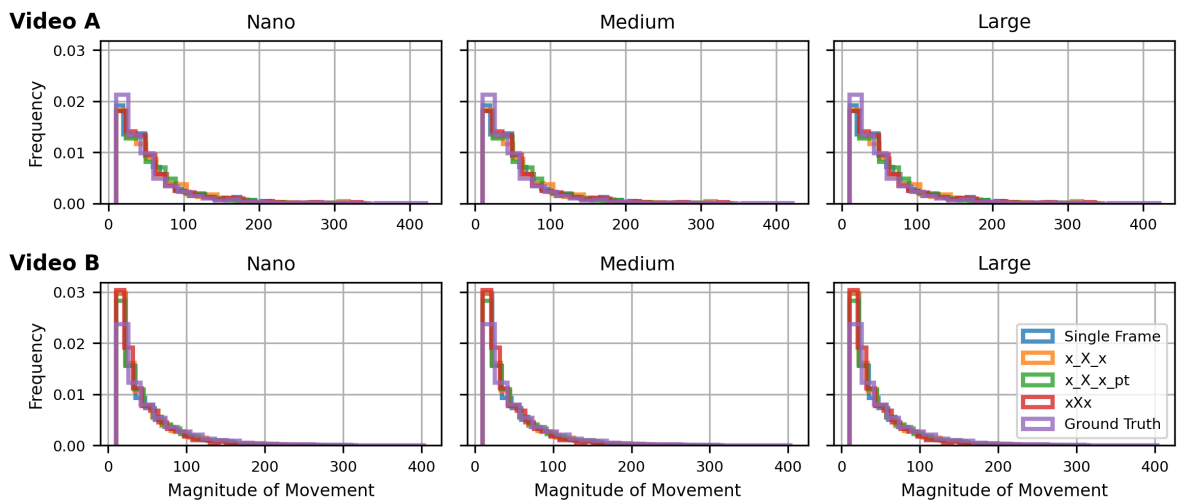


Figure 5: Histograms showing the aggregated magnitude of the swimming directions from tracking with model size nano (left), medium (middle) and large (right) for video A (top row) and video B (bottom row).

## 6 CONCLUSIONS

Quantitative features derived from fish movement can be important indicators for the fish health conditions in cultured environments. In particular, prominent vertical swimming behavior can reveal stress or pathology, potentially caused by e.g. electrical leakage current (Moccia, 1991). To assess the feasibility of inferring fish locomotion activity in aquarium settings, we constructed a MOT and segmentation dataset comprising shoals of *Sulawesi ricefish*.

We have shown that increasing the context window in YOLOv11 detection models improves detection accuracy with modest adaptations. Higher detection accuracy leads to more robust and consistent

tracking in Bytetrack and BoT-SORT tracking methods. Tracking on the ground-truth detections has shown that TbD are capable enough for accurate fish tracking. However, the results substantially depend on the fidelity of the detection, which are yet far behind the ground-truth.

For further evaluation, we plan to deploy our tracking system in a biodiversity-focused fish farm and analyze fish locomotion over an extended period of time. In addition, we will extend our tracking approach by estimating locomotion during the camera’s exposure time using concepts for explicit modeling of motion blur (Seibold et al., 2017).

Nevertheless, current TbD methods are sufficient to derive reliable quantitative estimates of shoal mo-

tion direction, and these measurements can therefore be used to draw conclusions about the fish's health status.

## ACKNOWLEDGEMENTS

This work was partly funded by the German Federal Ministry for Economic Affairs and Energy (FischFitPro, grant no. 16KN095536) and the Federal Ministry of Research, Technology and Space (RE-FRAME, grant no. 01IS24073A).

## REFERENCES

- Aharon, N., Orfaig, R., and Bobrovsky, B.-Z. (2022). BoT-SORT: Robust Associations Multi-Pedestrian Tracking. *arXiv e-prints*, page arXiv:2206.14651.
- Bernardin, K. and Stiefelwagen, R. (2008). Evaluating multiple object tracking performance: The clear mot metrics. *EURASIP Journal on Image and Video Processing*, 2008.
- Cui, M., Liu, X., Liu, H., Zhao, J., Li, D., and Wang, W. (2025). Fish Tracking, Counting, and Behaviour Analysis in Digital Aquaculture: A Comprehensive Survey. *Reviews in Aquaculture*, 17(1):e13001.
- Du, Y., Wan, J., Zhao, Y., Zhang, B., Tong, Z., and Dong, J. (2022a). GIAOTracker: A comprehensive framework for MCMOT with global information and optimizing strategies in VisDrone 2021. *arXiv e-prints*, page arXiv:2202.11983.
- Du, Y., Zhao, Z., Song, Y., Zhao, Y., Su, F., Gong, T., and Meng, H. (2022b). StrongSORT: Make DeepSORT Great Again. *arXiv e-prints*, page arXiv:2202.13514.
- Everingham, M., Eslami, S. M., Gool, L., Williams, C. K., Winn, J., and Zisserman, A. (2015). The pascal visual object classes challenge: A retrospective. *Int. J. Comput. Vision*, 111(1):98–136.
- Jocher, G. and Qiu, J. (2024). Ultralytics yolo11. <https://github.com/ultralytics/ultralytics>.
- Kalman, R. E. (1960). A new approach to linear filtering and prediction problems. *Journal of Basic Engineering*, 82(1):35–45.
- Khanam, R. and Hussain, M. (2024). YOLOv11: An Overview of the Key Architectural Enhancements. *arXiv e-prints*, page arXiv:2410.17725.
- Koller, D., Weber, J., and Malik, J. (1994). Robust multiple car tracking with occlusion reasoning. In Eklundh, J.-O., editor, *Computer Vision — ECCV '94*, pages 189–196, Berlin, Heidelberg. Springer Berlin Heidelberg.
- Leatherland, J. and Woo, P. (2006). *Fish Diseases and Disorders*. Number Bd. 2 in Fish Diseases and Disorders. CABI.
- Li, W., Li, F., and Li, Z. (2022). Cmftnet: Multiple fish tracking based on counterpoised jointnet. *Computers and Electronics in Agriculture*, 198:107018.
- Lin, T.-Y., Maire, M., Belongie, S., Bourdev, L., Girshick, R., Hays, J., Perona, P., Ramanan, D., Zitnick, C. L., and Dollár, P. (2014). Microsoft COCO: Common Objects in Context. *arXiv e-prints*, page arXiv:1405.0312.
- Liu, Y., Li, B., Zhou, X., Li, D., and Duan, Q. (2024). Fish-track: Multi-object tracking method for fish using spatiotemporal information fusion. *Expert Systems with Applications*, 238:122194.
- Luiten, J., Ošep, A., Dendorfer, P., Torr, P., Geiger, A., Leal-Taixé, L., and Leibe, B. (2020). Hota: A higher order metric for evaluating multi-object tracking. *International Journal of Computer Vision*, 129(2):548–578.
- Luo, W., Xing, J., Milan, A., Zhang, X., Liu, W., and Kim, T.-K. (2021). Multiple object tracking: A literature review. *Artificial Intelligence*, 293:103448.
- Moccia, R. D. (1991). Fish electrocution. OAC Publication 2191. Accessed: 5 January 2026.
- Quan, Y., Kiefer, B., Messmer, M., and Zell, A. (2025). Lightweight Multi-Frame Integration for Robust YOLO Object Detection in Videos. *arXiv e-prints*, page arXiv:2506.20550.
- Redmon, J., Divvala, S., Girshick, R., and Farhadi, A. (2016). You only look once: Unified, real-time object detection. *arXiv e-prints*, page arXiv:1506.02640.
- Ristani, E., Solera, F., Zou, R. S., Cucchiara, R., and Tomasi, C. (2016). Performance Measures and a Data Set for Multi-Target, Multi-Camera Tracking. *arXiv e-prints*, page arXiv:1609.01775.
- Roberts, J. (2023). *Swim Bladder Disease: How to Treat Swim Bladder Disease in Aquarium Fish*. Amazon Digital Services LLC.
- Seibold, C., Hilsmann, A., and Eisert, P. (2017). Model-based motion blur estimation for the improvement of motion tracking. *Computer Vision and Image Understanding*, 160:45–56.
- Wang, G., Yuan, Y., Chen, X., Li, J., and Zhou, X. (2018). Learning discriminative features with multiple granularities for person re-identification. In *Proceedings of the 26th ACM international conference on Multimedia*, MM '18, page 274–282. ACM.
- Wojke, N., Bewley, A., and Paulus, D. (2017). Simple online and realtime tracking with a deep association metric. In *2017 IEEE International Conference on Image Processing (ICIP)*, pages 3645–3649.
- Yang, B., Huang, C., and Nevatia, R. (2011). Learning affinities and dependencies for multi-target tracking using a crf model. In *CVPR 2011*, pages 1233–1240.
- Zhang, Y., Sun, P., Jiang, Y., Yu, D., Weng, F., Yuan, Z., Luo, P., Liu, W., and Wang, X. (2021). ByteTrack: Multi-Object Tracking by Associating Every Detection Box. *arXiv e-prints*, page arXiv:2110.06864.